DOI: 10.1002/anie.200802185

Anisotropic Nanoparticles

Imidazolium-Based Ionic Liquids as Efficient Shape-Regulating Solvents for the Synthesis of Gold Nanorods**

*Hyung Ju Ryu, Luz Sanchez, Heidrun A. Keul, Aanchal Raj, and Michael R. Bockstaller**

Dedicated to Professor Gerhard Wegner on the occasion of his 68th birthday

The tuneable NIR absorbance of gold in conjunction with its low cytotoxicity has fueled research in the synthesis of rodlike gold nanocrystals for a wide range of biomedical applications such as sensing, imaging, and photothermal therapy.[1] However, a fundamental problem in the realization of these technologies is the need for (cytotoxic) surfactants—such as cetyltrimethylammonium bromide (CTAB)—in order to induce the anisotropic particle growth in aqueous solution.[2] Herein we present an alternate synthetic strategy based on ionic liquid solvents that alleviates the need for shape-regulating surfactants.

Ionic liquids (ILs) have attracted interest as benign solvent systems for the synthesis of nanomaterials as they combine several attractive characteristics, for example inherent conductivity, stability over a broad range of electrochemical potentials, and environmental benefits deriving from the low vapor pressure and straightforward separation procedures.[3,4] Two major strategies have been pursued for the synthesis of metal nanoparticles in IL solution: 1) the addition of auxiliary capping agents (in analogy to the reactions in aqueous solution) to stabilize the formation of nanosized particles, and 2) the use of modified ILs capable of acting both as solvent and capping agent. For example, thiol- and alcohol-substituted ILs were applied for the synthesis of Au and Pt nanoparticles by reduction of the respective metal salts with a strong reducing agent ($NaBH_4$).[5,6] Common to these prior studies is the use of strong reducing agents and the (predominantly) covalent linkage of the capping agent to stabilize the growing metal nuclei.

[*] H. J. Ryu, A. Raj, Prof. Dr. M. R. Bockstaller
Department of Materials Science and Engineering
Carnegie Mellon University, 5000 Forbes Avenue
Pittsburgh, PA 15213 (USA)
Fax: (+1) 412-268-7247
E-mail: Bockstaller@cmu.edu
Homepage: http://neon.mems.cmu.edu/people/bockstaller.htm
L. Sanchez
Department of Physics and Astronomy, Hunter College, CUNY
695 Park Avenue, New York, NY 10021 (USA)
H. A. Keul
DWI and Institute of Technical and Macromolecular Chemistry
RWTH Aachen, Pauwelsstrasse 8, 52056 Aachen (Germany)

[**] Financial support from the National Science Foundation (grants DMR-0351770 and DMR-0706265) and the INTEL IFYRE program (A.R.) is gratefully acknowledged. H.K. and M.R.B. also acknowledge support by the German Science Foundation (grant Bo 1948/1-2). The authors thank Tom Nuhfer for his assistance in performing the high-resolution electron microscopy.

We report herein that under conditions of decelerated particle growth (by use of weak reducing agents) the stabilization of gold nanocrystals is facilitated by solvent coordination in unmodified imidazolium ionic liquids.[7,8] Imidazolium cations are particularly intriguing stabilizing agents for gold nanocrystals since related aromatic heterocycles have been shown to preferentially bind to high-energy crystallographic orientations of gold surfaces such as the {100}, {110}, and {311} orientations.[8–10] This suggests that imidazolium-based ILs may stabilize non-equilibrium particle shapes (such as nanorods) that exhibit fewer low-energy {111} facets than the equilibrium (Wulff) shape.

We demonstrate herein that anisotropic gold nanocrystals can be synthesized in 1-ethyl-3-methylimidazolium ethylsulfate ([EMIM][ES]) in very high yield in the absence of auxiliary shape-regulating surfactants. Dependent on the amount of Ag^I present in the reaction mixture, the particle aspect ratio can be controlled within the range $a = L/d = 1$–15 (where L and d denote the particle length and thickness); this is comparable to the range of shape anisotropy that has been demonstrated in aqueous solutions.

The synthetic approach is based on the seeded-growth method originally developed by the Murphy group for the synthesis of gold nanorods in aqueous surfactant systems[12–14] and takes advantage of the stabilization of Au^I in the presence of weak reducing agents in [EMIM][ES]. In a first step, spherical gold nanocrystals (seed crystals) are synthesized in IL solution ([EMIM][ES]) using strong reducing agents (trisodium citrate and/or sodium borohydride. Note that the reductive strength of borohydride exceeds that of citrate; however, for the purpose of the present paper, both will be considered as strong reducing agents). Subsequently the nanocrystals are injected into a "secondary-growth solution" comprising a solution of Au^I, Ag^I, and a weak reducing agent (ascorbic acid) in [EMIM][ES].[15] The reaction process is illustrated in Scheme 1.

[EMIM][ES] was chosen as the IL because of its hydrophilic characteristics and high dielectric constant ($\varepsilon = 27.9$) which supports the dissolution of inorganic salts.[16] Seed crystals of three different sizes were synthesized (by progressively increasing the amount of $NaBH_4$ during the reduction process) in order to elucidate the effect of seed crystal size on rod formation: $\langle d\rangle_{S1} = (9.4 \pm 4)$ nm, $\langle d\rangle_{S2} = (6.5 \pm 2.1)$ nm and $\langle d\rangle_{S3} = (3.9 \pm 1.6)$ nm. The Ag^I content in the growth solution was set at $x_{Ag} = 0$, 0.04, 0.08, and 0.16 (with $x_{Ag} = c(Ag^I)/c(Au^I)$ denoting the molar ratio of Ag^I) in order to elucidate the relevance of Ag^I on the rod-formation process.

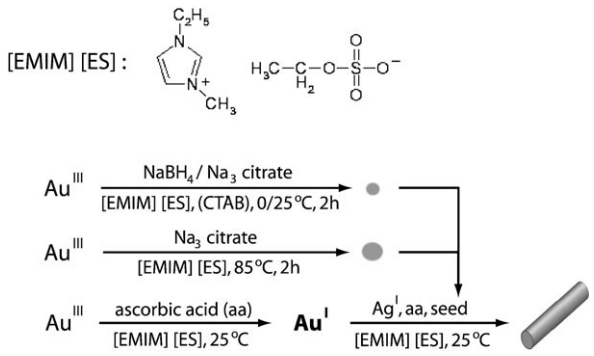

Scheme 1. Two-step synthesis of gold nanoparticles: Reduction of Au^{III} in [EMIM][ES] by (relatively) strong reducing agents (citrate and/or sodium borohydride) results in the formation of spherical crystals (seed crystals). The size of these seed crystals is controlled by the relative amount of $NaBH_4$. Addition of the weak reducing agent ascorbic acid stabilizes Au^{I} in [EMIM][ES] solution and facilitates anisotropic growth after addition of seed crystals.

Figure 1 depicts the optical absorption spectra of tenfold diluted samples of the nanorod solution recorded 2, 5, 10, and 30 minutes after the injection of seed crystals $\langle d\rangle_{S2} = (6.5 \pm 2.1)$ nm to a growth solution with $x_{Ag} = 0.08$. At short reaction times ($t = 2$ and 5 min) the absorption spectra are dominated by the damped plasmon resonance at $\lambda = 542$ nm that is characteristic of small spherical gold nanocrystals in [EMIM][ES]. After $t = 10$ minutes a distinct long-wavelength absorption at $\lambda = 725$ nm is observed, which becomes a dominant absorption peak at $\lambda = 749$ nm for the sample obtained after $t = 30$ minutes. This transition is indicative of the growth of anisotropic gold particles in which the splitting of the plasmon resonance in transverse and longitudinal excitation modes gives rise to the characteristic long-wavelength plasmon absorption.[15]

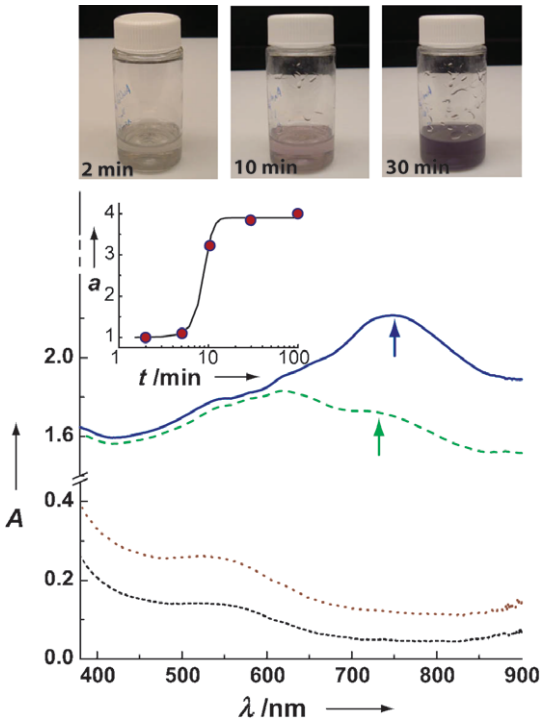

Figure 1. UV/Vis absorption spectra of nanorod solutions after reaction times of 2 (black), 5 (red), 10 (green), and 30 min (blue), along with photographs of the particle solutions. The increase and red-shift of the longitudinal plasmon resonance (indicated by arrows) from $\lambda = 725$ nm (10 min) to $\lambda = 749$ nm (30 min) is characteristic for anisotropic particle growth. The inset depicts the development of shape anisotropy a as function of time t as deduced from the optical spectra using Mie theory. The curve reveals a sigmoidal anisotropy evolution with maximum growth rate at $t \approx 10$ min. The line is introduced to guide the eye.

Growth of anisotropic particles is confirmed by transmission electron microscopy (TEM, Figure 2). After $t = 10$ minutes the formation of tadpole-type nanoparticles is observed with dimensions of $\langle d\rangle = (5 \pm 3)$ nm and $\langle L\rangle = (18 \pm 5)$ nm. With increasing reaction time t the average particle

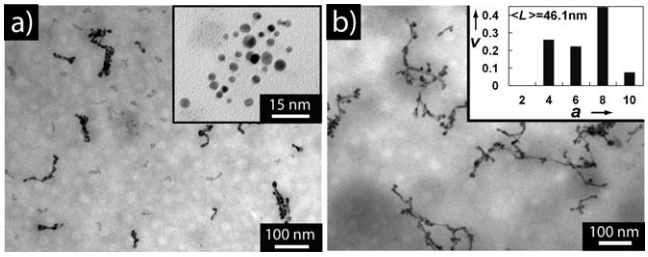

Figure 2. Bright-field TEM image of gold nanorods in [EMIM][ES] after different reaction times t. a) After $t = 10$ min, $\langle d\rangle = (5 \pm 3)$ nm and $\langle L\rangle = (18 \pm 5)$ nm; the inset shows seed nanocrystals ($\langle d\rangle_{S2} = (6.5 \pm 2.1)$ nm). b) After $t = 30$ min, $\langle d\rangle = (9 \pm 2)$ nm and $\langle L\rangle = (46.1 \pm 8)$ nm; the inset shows distribution of nanorod anisotropy a after $t = 30$ min (ν: normalized particle frequency).

shape anisotropy $\langle a\rangle$ (determined by electron microscopy) is found to increase to $\langle a\rangle \approx 6$ after $t = 30$ minutes Using model calculations based on Mie theory (not shown here) the wavelength for the longitudinal plasmon resonance can be estimated for gold nanorods with an aspect ratio $a = 6$ to be $\lambda_{th} \approx 900$ nm. This is somewhat larger than the $\lambda_{exp} = 749$ nm obtained from Figure 1 and suggests that TEM overestimates the average rod anisotropy by about 25%. The length disparity of nanorods evident from the micrograph (Figure 2b) also rationalizes the shoulder in the absorbance spectra after $t = 30$ minutes in the wavelength range $550 < \lambda < 700$ nm. No significant change in the optical characteristics of the particle solutions was observed after $t = 30$ minutes (supporting the sigmoidal development of particle aspect ratio deduced from the absorption spectra shown in Figure 1), and the solutions remained stable over two weeks—the maximum time considered in the experiments. Analysis of electron micrographs such as Figure 2 furthermore reveals a ratio of rodlike to spherical particle morphologies in excess of 9:1, indicating a high yield of rods.

Similar to previous reports on the synthesis of gold nanorods in aqueous surfactant solutions, rod formation was found be sensitive to the size of seed crystals; in other words, the rod anisotropy was found to progressively increase with decreasing seed crystal size (for constant x_{Ag}).[14,18] For example, at $x_{Ag} = 0.08$ no rod formation was observed for large seed crystals ($\langle d\rangle_{S1} = (9.4 \pm 3)$ nm), whereas small seed

particles ($\langle d\rangle_{S3} = (3.9 \pm 1.6)$ nm) resulted in nanorods with average anisotropy of $\langle a\rangle = 6.1$. We attribute the size dependence of the growth process to both kinetic and thermodynamic stabilization of large nanocrystals with the equilibrium shape.[19]

The presence of Ag^I during the growth process was found to be critical to induce the formation of nanorods. Figure 3 depicts the electron micrographs of nanorods that were synthesized using small seed crystals ($\langle d\rangle_{S3} = (3.9 \pm 1.6)$ nm) with progressively increasing molar fraction of Ag^I ($x_{Ag} =$ 0.04, 0.08, and 0.16 after $t = 30$ min). Both the particle anisotropy and nanorod yield (i.e. the number of rods relative to the total number of particles) are found to increase with increasing x_{Ag}. In the absence of Ag^I (i.e. $x_{Ag} = 0$) only spherical particles formed.

The relevance of Ag^I bears similarity to observations made with aqueous surfactant systems in which a small amount of Ag^I was found to support the formation of rodlike particle shapes. In aqueous systems it has been proposed that Ag^I contributes to the stabilization of non-equilibrium rodlike particle shapes through underpotential deposition and the formation of ad-layers on the gold crystal surface—presumably on the high-energy {110} and {100} facets that are prevalent in single-crystalline gold nanorods.[13,14] While the role of Ag^I cannot be resolved in the present study it is interesting to note that the results suggest the shape-regulating effect to be associated with Ag^I rather than AgBr which has been discussed as a possible contributor in the stabilization process in aqueous systems.

The micrographs shown in Figure 3 reveal a significant difference between the morphology of nanorods formed in [EMIM][ES] and those in aqueous surfactant solutions. Whereas in the latter case "ideal" rodlike single-crystalline or twinned morphologies have been observed, nanorods synthesized in [EMIM][ES] exhibit a more irregular head/tail-type geometry, in which the (presumably) seed nanocrystals ("head") can be distinguished from the attached "tail" of the rod.[14] To elucidate the origin for the difference in particle-shape evolution, high-resolution electron microscopy (HRTEM) was performed on nanorods after $t =$ 30 minutes (synthesized using seed crystals $\langle d\rangle_{S2} = (6.5 \pm$ 2.1) nm and $x_{Ag} = 0.08$; see also micrograph shown in Figure 2b). Figure 4 confirms the predominant single-crystallinity of the nanorods and reveals that the nanorods' growth direction is primarily along the $\langle 100\rangle$ direction. This suggests that the role of [EMIM][ES] in regulating the particle shape is similar to that of CTAB in aqueous solution, for which the anisotropic growth has been related to the higher binding affinity of the surfactant to the high-energy {100} and {110} crystal facets.[14]

Intriguing insight into the origin of the rather irregular rodlike shape of nanorods in [EMIM][ES] is provided by the HRTEM images shown in Figure 4b and 4c, which depict a profile view along [010] direction. The magnified profile view clearly reveals the "irregular" structure of the {100} rod facet resulting from atom-height surface steps (indicated by arrows in Figure 4c). The deviation of nanorod facets from the "ideal" atomically smooth atom arrangement as a consequence of surface relaxation and reconstruction processes was

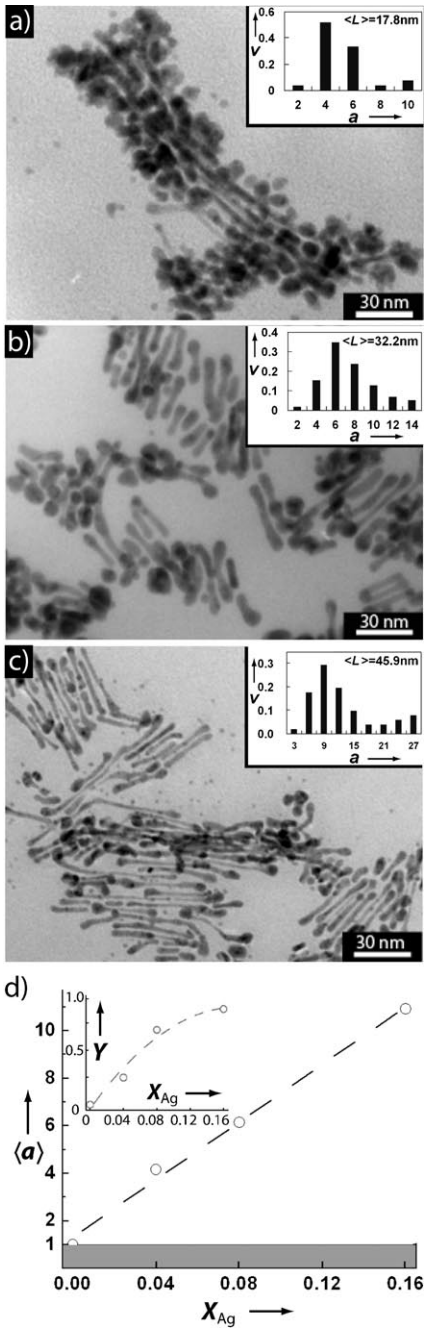

Figure 3. a–c) Bright-field TEM images of gold nanorods in [EMIM][ES] for different molar fractions of Ag^I at $t = 30$ min after addition of seed crystals $\langle d\rangle_{S3} = (3.9 \pm 1.6)$ nm. Insets depict the respective particle anisotropy distribution. a) $x_{Ag} = 0.04$, $\langle a\rangle = 4.2$. b) $x_{Ag} = 0.08$, $\langle a\rangle = 6.1$, $\langle L\rangle = (32.2 \pm 4.1)$ nm. c) $x_{Ag} = 0.16$, $\langle a\rangle = 10.9$, $\langle L\rangle = (45.9 \pm 6.2)$ nm. d) Plot of the average rod anisotropy as function of x_{Ag}; $\langle a\rangle$ is found to increase approximately linearly with x_{Ag}. The inset shows the increase in nanorod yield Y (defined as the number fraction of rodlike particles) with increasing x_{Ag}. Dashed lines are inserted to guide the eye.

first demonstrated by El-Sayed and co-workers using single-crystalline gold nanowires grown by electrolytic deposition.[20] Fundamentally, surface relaxation and reconstruction describe the process by which layers of atom planes in the vicinity of the surface assume spacings (relaxation) or

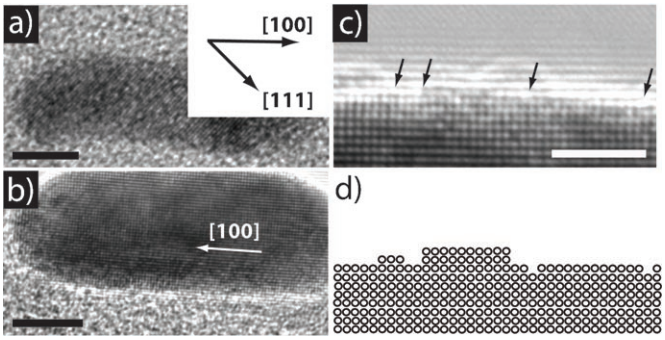

Figure 4. HRTEM images of gold nanorods grown in [EMIM][ES]: a) {111} sublattice (lattice distance: 0.236 nm) (scale bar: 5 nm) and b) {100} sublattice (scale bar: 5 nm). The micrographs reveal the single-crystalline structure and primary direction of particle growth along ⟨100⟩. Inset in (a) shows the respective crystallographic directions. c) Magnified [010] profile view, demonstrating the formation of atom-height surface steps along the (001) crystal facets. Arrows indicate location of surface steps (scale bar: 2 nm). d) Sketch showing the approximate atomic positions deduced from (c).

arrangements (reconstruction) that are different from those of atoms in the bulk in order to lower the overall free energy. While relaxation and reconstruction processes have received much attention in the study of planar metal surfaces, the implications on the growth of nanocrystals have only rarely been explored. Recently, Keul et al. demonstrated the occurrence of (1×2) missing-row reconstruction on {110} crystal facets of gold nanorods synthesized by the seeded-growth approach.[21] They postulated that surface reconstruction constitutes a competing mechanism during particle growth that is responsible for the transition from anisotropic to isotropic growth observed in aqueous nanorod solutions.[21] We hypothesize that the origin of the difference in particle shapes of nanorods synthesized in [EMIM][ES] and aqueous solution is related to subtle differences in the specific binding affinity of [EMIM][ES] and CTAB to the crystal facets (perhaps mediated by the formation of Ag ad-layers) which alter the respective surface reconstruction and relaxation processes. In particular, the frequency of surface-step irregularities of nanorod [010] facets as deduced from Figure 4c exceeds the numbers reported for nanorods in aqueous media, thus suggesting surface reconstruction to be more effective in [EMIM][ES] solution. It is conceivable that the more defective particle surface structure affects particle growth and results in more irregular morphologies. We note that this assertion is preliminary owing to the lack of sufficient statistics in HRTEM analysis; the change in solvent and surfactant will likely have a complex and multifaceted effect on the reaction process, including mass transport and thermodynamic driving force in addition to surface reconstruction processes.

In conclusion, the high-yield formation of rodlike gold nanoparticles in [EMIM][ES] in the absence of shape-regulating surfactants demonstrates new opportunities for IL solvent systems for the synthesis of nanomaterials. The size and shape of the nanoparticles is dictated by the preferential binding affinity of the imidazolium cations to low-density gold crystal facets when weak reducing agents are being used for particle growth. This could be of interest, for example, for the synthesis of gold nanorods for biomedical applications in which a fundamental problem persists in the cytotoxicity of the capping agents needed to induce the anisotropic growth. Since preliminary toxicological studies on imidazolium-based ionic liquids are encouraging, the IL-based synthesis approach could be more compatible with biomedical applications.[22]

Experimental Section

[EMIM][ES] (99%) was supplied by Alfa Aesar and dried in vacuum at 60°C for 48 h prior to use. $HAuCl_4$ (99.99%), $AgNO_3$ (99.99%), trisodium citrate (99%), $NaBH_4$ (99.99%), and ascorbic acid (99.9%) were obtained from Aldrich and used without further purification. All reactants were found to dissolve in [EMIM][ES] after stirring for 1 h and heating to $T=60$°C and to remain in solution after cooling to room temperature.

Citrate-capped seed nanocrystals with an average particle diameter of $\langle d\rangle_1=(9.4\pm3)$ nm were synthesized by addition of 0.5 mL of trisodium citrate (50 mM in [EMIM][ES]) to 5 mL of $HAuCl_4$ (1 mM in [EMIM][ES]). The solution was stirred for 120 minutes at 85°C before cooling to room temperature. Particle with sizes of $\langle d\rangle_2=(6.5\pm2.1)$ nm were synthesized by addition of 0.1 mM of $NaBH_4$ to the citrate solution in the presence of CTAB (0.3 mM). Particles with diameters of $\langle d\rangle_3=(3.9\pm1.6)$ nm were synthesized by addition of 0.5 mL of $NaBH_4$ (0.5 mL, 0.2 mM) to 5 mL of $HAuCl_4$ (1 mM in [EMIM][ES]) in the presence of CTAB (1 mM) at 0°C. The solution was stirred for 60 minutes at 0°C before heating to room temperature. A secondary-growth solution was prepared by addition of 30 μL of ascorbic acid (1M in [EMIM][ES]) to 2.5 mL solution of $HAuCl_4$ (5 mM in [EMIM][ES]). Addition of the reducing agent resulted in a color transition from yellow to transparent within 60 s, indicating the complete reduction of Au^{III} to Au^{I}. Au^{I} was found to be stable in [EMIM][ES] even in the presence of excess amounts of ascorbic acid. Ag^{I} was introduced into the growth solution by addition of 0, 12.5, 25, and 50 μL of $AgNO_3$ (40 mM in [EMIM][ES]) to 2.5 mL of the Au^{I} solution, corresponding to molar ratios of $x_{Ag}=c(Ag^{I})/c(Au^{I})=0$, 0.04, 0.08, and 0.16, respectively. In order to induce rod formation 12 μL of the seed solution was added to the secondary-growth solution under vigorous stirring at 25°C.

UV/Vis spectroscopy was performed using a CARY 500 spectrophotometer. Transmission electron microscopy (TEM) was performed using a JEOL 2000 FX microscope operating at 200 kV. Specimen preparation was by drop-casting tenfold-diluted particle solutions on amorphous carbon-coated copper grids. High-resolution TEM was performed using a Philips Tecnai microscope operating at 200 kV.

Received: May 9, 2008
Published online: August 19, 2008

Keywords: crystal growth · gold · ionic liquids · nanorods · shape regulation

[1] a) C. Burda, X. Chen, R. Narayanan, M. A. El-Sayed, *Chem. Rev.* **2005**, *105*, 1025; b) C. Burda, X. Chen, R. Narayanan, Y. Xia, N. J. Halas, *MRS Bull.* **2005**, *30*, 338; c) X. Huang, I. H. El-Sayed, W. Qian, M. A. El-Sayed, *J. Am. Chem. Soc.* **2006**, *128*, 2115; d) C. J. Murphy, A. M. Gole, S. E. Hunyadi, J. W. Stone, P. N. Sisco, A. Alkilany, B. E. Kinard, P. Hankins, *Chem. Commun.* **2008**, 544.

[2] a) R. Cortesi, E. Esposito, E. Menegatti, R. Gombari, C. Nastruzzi, *Int. J. Pharm.* **1996**, *139*, 69; b) T. Niidome, M.

Yamagata, Y. Okamoto, Y. Akiyama, H. Takahashi, T. Kawano, Y. Katayama, Y. Niidome, *J. Controlled Release* **2006**, *114*, 343.
[3] a) I. Krossing, J. M. Slattery, C. Daguenet, P. J. Dyson, A. Oleinikova, H. Weingärtner, *J. Am. Chem. Soc.* **2006**, *128*, 13427; b) J. Dahl, B. L. S. Maddux, J. E. Hutchison, *Chem. Rev.* **2007**, *107*, 2228.
[4] M. C. Kroon, J. van Spronsen, C. J. Peters, R. A. Sheldon, G. J. Witkamp, *Green Chem.* **2006**, *8*, 246.
[5] a) K. S. Kim, D. Demberelnyamba, H. Lee, *Langmuir* **2004**, *20*, 556; b) R. Tatumi, H. Fujihara, *Chem. Commun.* **2005**, 83; c) C. W. Scheeren, G. Machado, S. R. Teixiera, J. Morais, J. B. Domingos, J. Dupont, *J. Phys. Chem. B* **2006**, *110*, 13011; d) K.-S. Kim, S. Choi, J.-H. Cha, S.-H. Yeon, H. J. Lee, *Mater. Chem.* **2006**, *16*, 1315.
[6] H. Itoh, K. Naka, Y. Chujo, *J. Am. Chem. Soc.* **2004**, *126*, 3026.
[7] Imidazolium-based ionic liquids have been used to stabilize sputter-deposited Au^0 particles, however, in the absence of reducing agents (see Ref. [8]).
[8] K. Okazaki, T. Kiyama, K. Hirahara, N. Tanaka, S. Kuwabata, T. Torimoto, *Chem. Commun.* **2008**, 691.
[9] a) L. Stolberg, J. Lipowski, *J. Electroanal. Chem.* **1987**, *238*, 333; b) A. Iannelli, J. Lipowski, *J. Phys. Org. Chem.* **2003**, *16*, 675.
[10] The preferred coordination of N heterocycles to the low-density surface orientations of Au has been related to the parallel coordination of the aromatic ring. See Ref. [9].
[11] a) V. O. Santos Jr. , M. B. Alves, M. S. Carvalho, P. A. Z. Suarez, J. C. Rubin, *J. Phys. Chem. B* **2006**, *110*, 20379; b) H. S. Schrecker, M. A. Gelesky, M. P. Stracke, C. M. L. Schrecker, G. Machado, S. R. Teixeira, J. C. Rubim, J. Dupont, *J. Colloid Interface Sci.* **2007**, *316*, 189.
[12] a) N. R. Jana, L. Gearheart, C. J. Murphy, *J. Phys. Chem. B* **2001**, *105*, 4065; b) N. R. Jana, L. Gearheart, C. J. Murphy, *Adv. Mater.* **2001**, *13*, 1389.
[13] The detailed mechanism of anisotropic particle growth using the method described in Ref. [12] is not resolved; however, it has been proposed that the preferential binding of the surfactant (CTAB) to the high-energy crystal facets (in conjunction with slow reaction kinetics and the formation of Ag ad-layers) provides a "symmetry-breaking" mechanism that induces the anisotropic growth of FCC gold. See also Ref. [14].
[14] a) M. A. El-Sayed, B. Nikoobakht, *Chem. Mater.* **2003**, *15*, 1957; b) C. J. Murphy, T. K. Sau, *Langmuir* **2004**, *20*, 6414; c) N. R. Jana, L. Gearheart, C. J. Murphy, *Adv. Mater.* **2001**, *13*, 1389; d) J. Pérez-Juste, L. M. Liz-Marzan, S. Carnie, D. J. C. Chan, P. Mulvaney, *Adv. Funct. Mater.* **2004**, *14*, 571; e) J. Chen, B. J. Wiley, Y. Xia, *Langmuir* **2007**, *23*, 4120; f) M. Liu, Guyot-Sionnest, *J. Phys. Chem. B* **2005**, *109*, 22192.
[15] Nanorod formation was also observed when seed crystals were synthesized in aqueous solution using CTAB as the stabilizing agent.
[16] H. Weingärtner, *Angew. Chem.* **2008**, *120*, 664; *Angew. Chem. Int. Ed.* **2008**, *47*, 654.
[17] U. Kreibig, M. Vollmer, in *Optical Properties of Metal Clusters*, *Vol. 25*, Springer, New York, **1995**, Springer Series in Materials Science.
[18] N. R. Jana, *Small* **2005**, *1*, 875.
[19] J. L. Elechiguerra, J. Reyes-Gasga, M. J. Yacaman, *J. Mater. Chem.* **2006**, *16*, 3906.
[20] Z. L. Wang, R. P. Gao, B. Nikoobakht, M. A. El-Sayed, *J. Phys. Chem. B* **2000**, *104*, 5417.
[21] H. Keul, M. Möller, M. R. Bockstaller, *Langmuir* **2007**, *23*, 10307.
[22] J. Ranke, S. Stolte, R. Stormann, J. Arning, B. Jastorff, *Chem. Rev.* **2007**, *107*, 2183.

